Rnf2 (*Ring1b*) deficiency causes gastrulation arrest and cell cycle inhibition

Jan Willem Voncken*†, Bernard A. J. Roelen‡§, Mieke Roefs*, Stijn de Vries*, Els Verhoeven*, Silvia Marino¶, Jacqueline Deschamps‡, and Maarten van Lohuizen*‖

*Division of Molecular Genetics, The Netherlands Cancer Institute, 1066 CX Amsterdam, The Netherlands; ‡Hubrecht Laboratory, The Netherlands Institute for Developmental Biology, 3584 CT Utrecht, The Netherlands; and ¶Institute of Clinical Pathology, University Hospital, CH-8091 Zürich, Switzerland

Edited by Stanley J. Korsmeyer, Dana–Farber Cancer Institute, Boston, MA, and approved December 23, 2002 (received for review July 19, 2002)

The highly homologous Rnf2 (Ring1b) and Ring1 (Ring1a) proteins were identified as *in vivo* interactors of the Polycomb Group (PcG) protein Bmi1. Functional ablation of *Rnf2* results in gastrulation arrest, in contrast to relatively mild phenotypes in most other PcG gene null mutants belonging to the same functional group, among which is *Ring1*. Developmental defects occur in both embryonic and extraembryonic tissues during gastrulation. The early lethal phenotype is reminiscent of that of the PcG-gene knockouts *Eed* and *Ezh2*, which belong to a separate functional PcG group and PcG protein complex. This finding indicates that these biochemically distinct PcG complexes are both required during early mouse development. In contrast to the strong skeletal transformation in *Ring1* hemizygous mice, hemizygocity for *Rnf2* does not affect vertebral identity. However, it does aggravate the cerebellar phenotype in a *Bmi1* null-mutant background. Together, these results suggest that Rnf2 or Ring1-containing PcG complexes have minimal functional redundancy in specific tissues, despite overlap in expression patterns. We show that the early developmental arrest in *Rnf2*-null embryos is partially bypassed by genetic inactivation of the *Cdkn2a* (*Ink4a*/*ARF*) locus. Importantly, this finding implicates Polycomb-mediated repression of the *Cdkn2a* locus in early murine development.

Polycomb Group (PcG) proteins and their genetic counterparts, the trithorax Group proteins (trxG), maintain *Hox* gene expression boundaries (1–4), which are critical for regional patterning along the antero-posterior (AP) axis (5–7). Based on biochemical characteristics, mammalian PcG proteins are currently grouped into at least two distinct functional groups: the first comprises Eed, Ezh1, and Ezh2 in the mouse (8, 9); the second consists of the highly related protein pairs Cbx2 (M33)/Cbx4 (MPc2), Bmi/Zfp144 (Mel18), and Edr1 and 2 (Rae28/Mph1 and 2), respectively (10, 11). For ease of this discussion we refer to them as groups I and II, respectively. Group I and II homologs are evolutionarily conserved from *Drosophila* to humans, only group I homologs are found in plants and *Caenorhabditis elegans* as well, supporting the concept of separate function (12, 13). In addition, complex composition differs throughout development in a temporal and cell-type-specific manner (14, 15). Interaction of Eed with histone deacetylases and the intrinsic histone methyltransferase activity of Ezh proteins suggest mechanisms for repression by group I complexes (16–19). Although a mammalian hPRC-H (group II) complex harbors an intrinsic capacity to stabilize a repressive chromatin structure and counteract SWI/SNF chromatin remodeling complexes *in vitro*, its *in vivo* mode of action is not well understood (20). Association with histone methyl transferase activity may in part help explain the repressive action of some group II complexes (21).

Rnf2 and Ring1 have been identified as *in vivo* interactors of the group II PcG protein Bmi1 by us and others (22). These Ring finger proteins interact with a number of known class II PcG proteins, suggesting a central position in complex formation (refs. 22–24 and this study). To address the role of *Rnf2* in mammalian development, an *Rnf2* null-mutant mouse was generated. We find that in contrast to the reported relatively mild phenotypes observed in other group II PcG-gene null mutants, the *Rnf2* mutants display early developmental arrest, which also is observed for *Eed* and *Ezh2* knockout (KO) mice. We further show a partial bypass of the early embryonic arrest by genetic inactivation of the *Cdkn2a* tumor suppressor locus. Together, our results highlight an essential function for both group I and II Polycomb repressors during early mammalian development.

Materials and Methods

Yeast Two-Hybrid Assay. Two independent yeast two-hybrid screens were carried out as described elsewhere (9). Yeast strains Y190 and MAV103, which carry Gal4-inducible *HIS3* and *lacZ* reporter genes, were transformed with *Bmi1*-Ring finger encoding sequences (1–780) carrying a C-terminal Gal4 DNA binding domain (DBD). Bait-transformed yeast strains were transformed with a human Jurkat T cell cDNA library or a B cell cDNA library fused to Gal4-transactivation (TA) domain sequences.

Genomic Library Screens and Targeting Construct. The incomplete human *Rnf2* cDNA was used to screen a 129/Ola mouse genomic phage library. Two ≈18-kb overlapping fragments were used to design a targeting construct. The position of exons encoding the Ring finger domain was determined by standard single stranded ^{32}P-labeled oligonucleotide hybridization. A ±3.0-kb *Eco*RI–*Xho*I fragment containing sequences encoding the major part of the Ring finger domain was replaced by a neomycin selection cassette. Linearized gel-purified targeting vector DNA was electroporated into 129/Ola embryonic stem (ES) cells, which were selected on geneticin (G418) medium. DNA from individual G418-resistant ES cells colonies was *Bam*HI- or *Hin*dIII-digested and analyzed by Southern hybridization with a 5′-prime external probe and internal *Rnf2*-derived and neomycin-based probes. Two independent, correctly targeted ES cells were injected into FVB blastocysts.

***In Situ* Hybridization.** The hybridization of embryo sections with ^{35}S-labeled probes was carried out as originally described (25) by using modifications reported previously (26). The *Brachyury T*, *Hoxb1*, and *Evx-1* probes were transcribed from a 1.9-kb *Eco*RI genomic and an 800-bp and a 588-bp cDNA fragment, respectively. Whole-mount *in situ* hybridization with a 1-kb mCer1 probe was carried out as described (27).

Cell Culture and Immunoprecipitation. PcG cDNAs were cloned into pBABE (28) or LZRS-based (29) retroviral expression vectors. *Cbx2* (*M33*) and *Cbx4* (*MPc2*) were cloned into pMT-hemagglutinin (HA) plasmids; *Myc-Rnf2* (*Ring1b*) and HA-*Ring1* (*Ring1a*) and HA-*Eed* were cloned into pBABE-

This paper was submitted directly (Track II) to the PNAS office.

Abbreviations: PcG, Polycomb Group; ES cell, embryonic stem cell; E*n*, embryonic day *n*; KO, knockout; dKO, double KO; HE, heterozygous; TAP, tandem affinity purification; HA, hemagglutinin.

†Present address: Department of Molecular Genetics, University of Maastricht, 6200 MD, The Netherlands.

§Present address: Division of Cellular Biochemistry, The Netherlands Cancer Institute, 1066 CX Amsterdam, The Netherlands.

‖To whom correspondence should be addressed. E-mail: m.v.lohuizen@nki.nl.

www.pnas.org/cgi/doi/10.1073/pnas.0434312100

puromycin vector; *Bmi1*-PY, myc-*Ezh* and HA-*Ezh* were cloned into a LZRS-IRES-GFP plasmid. *Rnf2* (*Ring1b*)-tandem affinity purification (TAP) fusions (30) were generated in a LZRS-IRES-GFP vector. Cells were harvested and PcG complexes were extracted by using a method described elsewhere (10). Immunoprecipitations were carried out with IgG beads or, as indicated, with antisera against cellular PcG proteins. Protein detection was done by standard Western analysis.

Reverse Transcription, Amplification, and Sequencing. Individual embryonic day (E)7.5, pairs of E6.5, or 30 E3.5 embryos were transferred to clean tubes and snap-frozen on dry ice. For comparison, total RNA was extracted from $\approx 5 \times 10^3$ ES cells. RNA extraction was done as described (31), adapted to minute amounts (32). Reverse transcription (RT) was performed according to the manufacturer's specifications (SuperScript, GIBCO/BRL). Typically 0.15 (E7.5), 0.3 (E6.5), or 4.5 (E3.5) embryo equivalent was used in a subsequent PCR in PcG-cDNA amplification; RT-PCR of *β-Actin* served as an mRNA quality control. Semiquantitative RT-PCR was carried out as described (33); amplified products were detected by radiolabeled oligonucleotides. Reverse transcription and PCR conditions and amplimer sequences are available on request. Reverse transcribed, PCR-amplified total RNA from an *Rnf2*-heterozygous (HE) embryo was used to sequence the mRNA transcribed from the KO allele by using a Big-Dye Terminator method (Applied Biosystems) on an automated sequencing apparatus (ABI Prism 3700 DNA Analyzer, Applied Biosystems).

Histological and Skeletal Analysis. Whole mouse brains were fixed in 4% paraformaldehyde. Four-micrometer sagittal, paraffin-embedded sections were stained with hematoxylin and eosin (H&E). Immunohistochemistry for glial fibrillary acidic protein (GFAP; polyclonal, 1:500; Dako), NeuN (monoclonal, 1:4,000; Chemicon), and calbindin (polyclonal, 1:200; Chemicon) was done. Biotinylated secondary antibodies (goat anti-rabbit and rabbit anti-mouse; Dako) were used at a dilution of 1:300. Chromogens used for visualization were biotin/avidin-peroxidase (Dako) and diaminobenzidine. Skeletal phenotypes of newborn *Rnf2*/*Bmi1* compound mutant mice were determined as described (34).

Animal Procedures and Genotyping. Chimeric *Rnf2*-HE mice were backcrossed to a 129/Ola or FVB background. 129/Ola *Rnf2*-HE or second-generation FVB-backcrossed *Rnf2*-HE animals were intercrossed to obtain full *Rnf2*-KO mice. *Rnf2*-HE/*Bmi1*-HE (35) mice were backcrossed to a FVB background for at least four generations, as were *Rnf2*-HE/*Cdkn2a*-KO (36) animals. Embryos until E7.5 from timed pregnancies (E0.5 at noon) were used entirely for DNA or RNA isolation. Surrounding membranes were used for genotyping older embryos. *Rnf2*-HE intercrosses yielded 19 litters comprising in total 272 analyzed embryos. In total six litters, comprising 65 embryos, were analyzed in the *Rnf2*/*Cdkn2a*-double KO (dKO) background. The *Rnf2* genotype was determined by Southern analysis or PCR. *Bmi1* and *Cdkn2a*-WT and KO alleles were analyzed by PCR as described (33).

Results and Discussion

Null Mutation of *Rnf2* (*Ring1b*) Causes Early Developmental Arrest. By using yeast two-hybrid assays with the murine Bmi1 Ring finger domain and directly flanking sequences as bait, several positive, overlapping human cDNAs were identified as two previously characterized Ring finger proteins, Ring1 (Ring1a) and Rnf2 (22, 23). To study the role of Rnf2 in mammalian development, a replacement vector was used to interrupt the murine *Rnf2* locus in ES cells (Fig. 1*a*). Absence of functional *Rnf2* mRNA was confirmed by RT-PCR (see below; Figs. 1*c* and 3*d*). No null-mutant mice were detected among 101 10-day-old offspring and newborns tested, suggesting embryonic death. Indeed, the *Rnf2*-KO genotype was not detected beyond E10.5; Southern analysis did reveal the

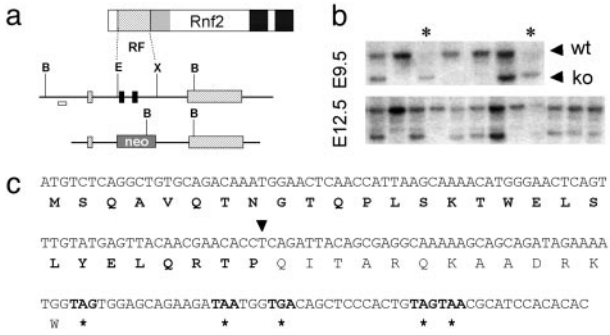

Fig. 1. Null mutation of the *Rnf2* locus. (*a*) *Rnf2* targeting construct. A ±3.0-kb *Eco*RI–*Xho*I 129/Ola genomic fragment containing exons (black boxes) encoding the major part of the Ring finger (RF) domain was replaced by a neomycin selection cassette. Shaded boxes indicate the approximate position of additional exons. (*b*) Early detection of the *Rnf2*-KO genotype. *Rnf2*-KO embryos are present during early development until E9, but not beyond E10. Genomic DNA was analyzed by *Bam*HI digestion and hybridization to an external 5′ probe indicated by the white box in *a*. (*c*) Functional null mutation of *Rnf2* gene. Total RNA isolated from an *Rnf2*-HE embryo was reverse transcribed and PCR sequenced. A shorter RT-PCR product (see Fig. 3*d*) potentially encodes a small peptide of 41 aa, of which only the N-terminal-most 28 residues correspond to Rnf2; arrowhead indicates the aberrant fusion point within the *Rnf2*-KO mRNA.

presence of *Rnf2*-KO embryos at E9.0–E9.5 at the expected 1 in 4 Mendelian ration (Fig. 1*b*). These observations held for two independently derived mouse lines in both the FVB and 129/Ola genetic background. E6.5, E7.5, and E8.5 null-mutant embryos all displayed an abnormal morphology, compared with that of WT and HE embryos. All *Rnf2*-KO embryos were delayed in development. Phenotypic variation was considerable: some KO concepti ($\approx$10%) displayed an "empty" parietal yolk sac (data not shown), most had progressed further, but lagged in development behind the controls, never reaching the headfold stage (Fig. 2*a*).

***Rnf2* Is Essential for Normal Gastrulation.** *Rnf2*-KO embryos do not progress through gastrulation normally (E6.5–E7; Fig. 2*b*). The lethal effect of *Rnf2*-inactivation is surprising, because null mutation of genes encoding other PcG complex members and/or binding partners revealed redundancy between highly related homologs (35, 37–41). Interestingly, genetic inactivation of *Eed* or *Ezh2*, both group I PcG proteins, results in gastrulation arrest as well (42, 43). *Eed* mutants arrest early, at least in part because Eed is necessary for stable maintenance of imprinted X inactivation in trophectoderm (44). Proper epiblast expansion also fails in these null-mutant embryos, possibly as a result of excessive ingression through the posterior primitive streak (45, 46); an excess of mesoderm localizes to the extraembryonic compartment, which may be caused by an anterior migration defect. *Ezh2* null mutant embryos either do not initiate or fail to complete gastrulation. Growth of the inner cell mass and epiblast cells is impaired and accumulation of mesoderm in the extraembryonic compartment was reported (43). We analyzed E6.5 through E8.5 *Rnf2*-KO embryos histologically and regarding expression of developmental markers. The data show that some *Rnf2*-KO embryos exhibit an abnormal distal restriction of the anterior visceral endoderm (AVE) marker *Cer1* (47) (Fig. 2*b*, rightmost embryo), whereas others show the normal anterior expression (Fig. 2*b*). These variations in Cer1 expression possibly reflect the considerable phenotypic variation observed in *Rnf2*-KO embryos.

In comparison to WT E7.5 embryos, a relatively far progressed *Rnf2*-KO reveals mesoderm accumulation in the primitive streak region posteriorly, but very little anteriorly expanding embryonic mesoderm (Fig. 2*c A* and *B*). Development of both the embryonic and extraembryonic part of the *Rnf2*-KO embryo is delayed. In particular, the posterior amniotic fold has

DEVELOPMENTAL BIOLOGY

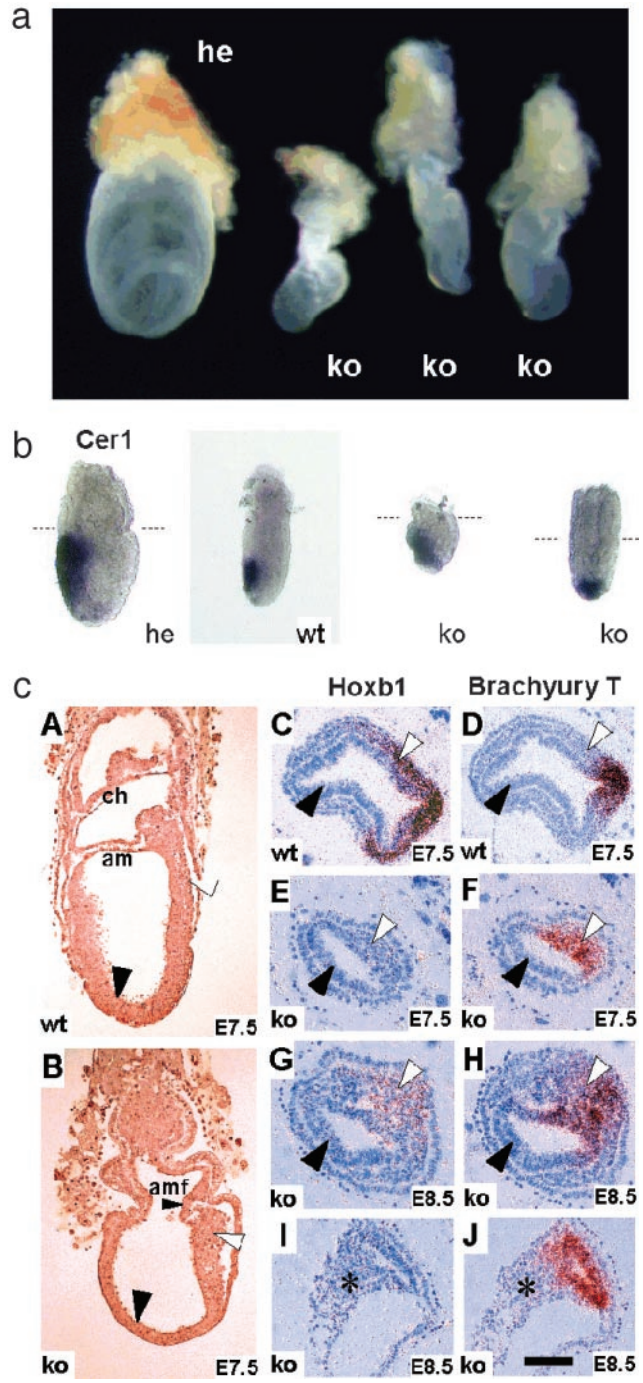

Fig. 2. Morphological abnormalities of *Rnf2*-KO embryos. (*a*) A normal day-7.5 embryo (*Left*) at the late headfold stage; neural folds are visible. Three smaller *Rnf2*-KO embryos (*Right*) manifest a characteristic phenotype. (*b*) Gene expression analysis in pre/early streak stage embryos (E6.2). The *Rnf2*-HE embryo is at early streak stage; the WT and KO embryos are prestreak. The early anterior visceral endoderm (AVE) marker *Cer1* is expressed in all *Rnf2* genotypes. *Cer1* expression is normally restricted in the KO embryo on the left, whereas it is abnormally localized in the KO on the right. Posterior is to the right; marker line: boundary extraembryonal (up)/embryonal tissue. (*c*) Histological and gene expression analysis of *Rnf2*-KO embryos confirms a significant delay in embryonic development. Posterior is to the right (*A–D*) or to the upper right (*E–J*); embryonic mesoderm (white arrowhead), embryonic ectoderm (black arrowhead), and allantois (asterisk) are indicated. (*A* and *B*) Sagittal sections of embryos at E7.5. Mesoderm has expanded all around the WT egg cylinder (*A*). am, amnion; ch, chorion. *Rnf2*-KO embryos show improper epiblast elongation and accumulation of posterior mesoderm (*B*). amf, posterior amniotic fold. (*C–J*), Transverse sections of embryos analyzed for *Hoxb1* (*C*, *E*, *G*, and *I*) and *Brachyury T* (*D*, *F*, *H*, and *J*) gene expression at E7.5 (*C–F*) and E8.5 (*G–J*). Sections *G–J* are from the same embryo; sections *H*, *G*, *J*, and *I* are progressively more proximal, with *J* being at a level passing through the base of the allantois and transecting the proximo-posterior part of the amniotic cavity (the amnion is closed). *Hoxb1* expression at E7.5 (*C* and *E*) is not yet initiated in the homozygous mutant embryo (*E*), whereas it is expressed in the posterior epiblast along the primitive streak and in nascent mesoderm in the WT (*C*; ref. 61). *Brachyury T* (*D* and *F*) is expressed in the mesoderm and ectoderm of the primitive streak in both WT and KO embryos, although it is weaker in the latter. (*G–J*) In E8.5 *Rnf2*-KO embryos (*G* and *I*) *Hoxb1* is expressed in the accumulated posterior mesoderm and in the ectoderm of the primitive streak (*G*) but not in extraembryonic mesoderm of the allantois (*I*); *Hoxb1* expression does not extend until the anterior end of the primitive streak. A weaker *Brachyury T* expression is visible in the epiblast and nascent mesoderm of the primitive streak (*H*) and in extraembryonic mesoderm at the base of the allantois (*J*) of the *Rnf2*-KO embryo. Note the posterior accumulation of mesoderm in the KO embryo (*G* and *H*). (Bar in *J*, ±0.1 mm.)

hardly formed in KO embryos (Fig. 2*cB*), whereas in WT and HE embryos, it has developed posteriorly and fused with anterior extraembryonic ectoderm, ensuring amnion and chorion formation (Fig. 2*cA*). In most cases, the chorion appeared abnormal (data not shown). Analysis of expression patterns *in situ* on transverse sections of *Rnf2*-KO embryos reveals that *Hoxb1*, one of the earliest *Hox* genes activated, is not expressed in E7.5 KO embryos (Fig. 2*cE*), whereas it is expressed at the proper location in the E8.5 KO, in the accumulated mesoderm and epiblast at the level of the primitive streak (Fig. 2*cG*). However, expression of *Hoxb1* in these tissues is significantly lower in E8.5 KO than in E7.5 controls (Fig. 2*c G* and *C*), in accordance with the severe developmental delay of the null mutants. The expression of the nascent mesoderm marker *Brachyury T* (Fig. 2*c D*, *F*, *H*, and *J*) and the posterior marker *Evx-1* (data not shown) is correctly restricted, but *T* expression is weaker in the E7.5 KO than in controls (Fig. 2*c D* and *F*). The developmental stage of the E8.5 KO shown in Fig. 2*c G* and *H* is closer to that of an E7.5 (Fig. 2*c C* and *D*) than to an E8.5 WT embryo (the latter not shown in these sections). Taken together, the above data illustrate a considerable delay in embryonic and extraembryonic development in *Rnf2*-KO embryos (cf. Fig. 2*a*).

PcG Gene Expression Profiles Are Not Affected by *Rnf2* Null Mutation. To substantiate that the null phenotype is not caused by altered expression of *Eed* or *Ezh2*, we studied the expression profiles of different PcG genes in early WT and KO embryos. *Rnf2* expression is detectable in blastocysts and ES cells, whereas *Eed* expression first appears shortly after implantation (Fig. 3*d*). This finding suggests that functional inactivation of *Eed* is unlikely to affect *Rnf2* expression at preimplantation stages. Vice versa, *Rnf2*-KO embryos still express the *Eed* (Fig. 3*d*). The expression profiles of *Ezh1* and *Ezh2* are unchanged in the absence of Rnf2, as is the case for *Ring1* and *Bmi1* (Fig. 3*d*). Also, under the indicated experimental conditions (i.e., approximately equal material input; see *Materials and Methods*), *Ring1* expression, in contrast to *Rnf2*, was not detectable in ES cells or blastocysts (Fig. 3*d*). Although more concentrated ES cell lysates reveal a low level of Ring1 expression (E. Boutsma and M.v.L., personal communication), the low levels of Ring1 detected clearly cannot compensate for the loss of Rnf2, both in ES cells and at later developmental stages. This observation further suggests a remarkable degree of functional divergence and specialization among highly related PcG proteins. The finding that compound null mutants for both Zfp144 (Mel18) and Bmi1 arrest later (i.e., at the 18th somite stage) than Rnf2 null mutants (41) further corroborates the notion of lineage-specific and temporal divergence among PcG complexes in murine development.

Because of temporally distinct expression profiles in early development, Ezh2-mediated silencing is thought to occur even before the onset of *Eed* expression (43). Likewise, *Rnf2* is expressed

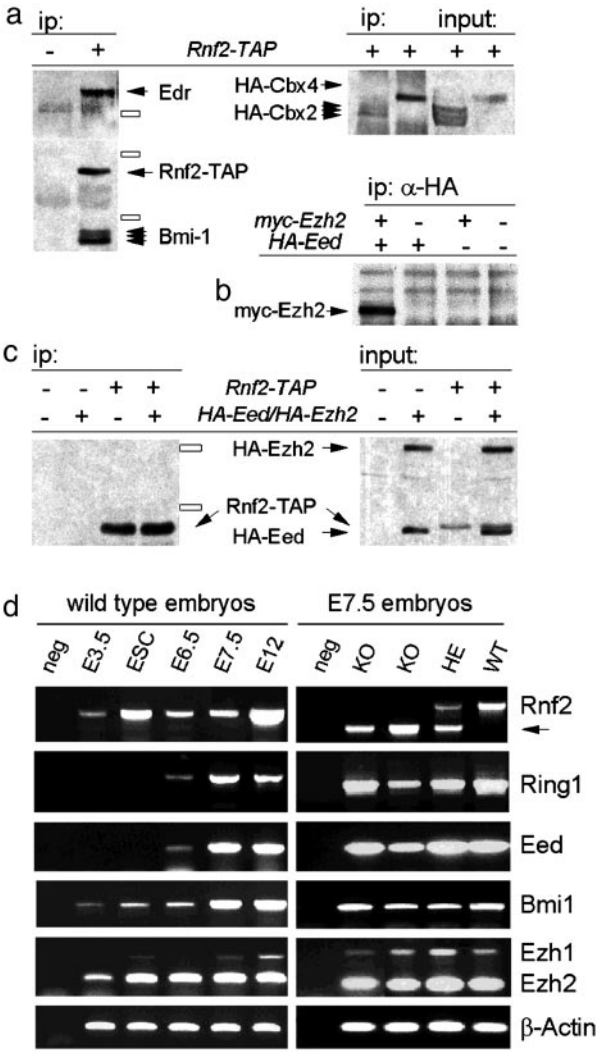

Fig. 3. Rnf2 interactions in whole cells and early embryonic PcG expression profiles. (*a*) Cotransfection experiments demonstrate interaction of *Rnf2*-TAP-tag with HA-tagged Cbx2 (M33) and Cbx4 (MPc2) in COS-7 cells (*Right*) and with endogenous Bmi1 and Edr (Mph) in human U2-OS osteosarcoma cells (*Left*). Size markers: 97, 66, and 46 kDa. (*b*) Coimmunoprecipitation of myc-Ezh2 with HA-Eed from transfected U2-OS cell extracts shows interactions between class I PcG members. (*c*) TAP-tagged *Rnf2* does not interact with HA-Eed or HA-Ezh2 in U2-OS cells (*Left*). Size markers: 97 and 66 kDa. (*d*) PcG gene expression profiles during early murine development. RT-PCR was done on total RNA from WT blastocysts (E3.5), ES cells (ESC), and E6.5, E7.5, and E12.5 embryos (*Left*). The expression profiles of *Rnf2*, *Ring1* (*Ring1a*), *Bmi1*, *Eed*, *Ezh1*, and *Ezh2* genes are shown. *β-Actin* serves as a qualitative control. (*Right*) PcG gene expression is not altered in *Rnf2*-KO embryos. Expression analysis in WT, HE, and KO E7.5 embryos. The shorter *Rnf2*-KO transcript (arrow) is the result of a deletion of exons encoding the major part of the Ring finger (see Fig. 1*c*).

relatively early and at a higher level than some of its binding partners, such as Bmi1. The observation that robust embryonic expression of *Rnf2* appears to precede *Eed* also may suggest that early PcG-mediated repression functions in part by means of a mechanism independent of Eed-mediated histone deacetylase recruitment.

Differences in PcG Complex Composition in Early Mammalian Development. We next studied PcG protein interactions in whole cells. Rnf2 is readily detectable in complex with mammalian group II PcG proteins (e.g., Bmi1, Cbx2, Cbx4, and Edr; Fig. 3*a*). The phenotypic resemblance of group I and *Rnf2* null mutants prompted us also to study Rnf2–group I PcG interactions. We found that Rnf2 does not interact with Eed or Ezh2 in several differentiated, established cell lines, as examined by coexpression and immunoprecipitation (Fig. 3 *b* and *c*). Although these findings are in full agreement with recent reports by other laboratories (8, 9, 22–24), we cannot formally exclude that experimental conditions used so far do not permit detection of a more transient interaction between group I and group II complexes (see discussion below). Alternatively, group I/II interactions may be cell-type-specific or mediated by as-yet-unknown cellular factors in early murine development.

Compound Group-II PcG Mutations Reveal Genetic Interaction but also Suggest Divergences in Target Genes. Although a hypomorphic *Rnf2* mutant causes subtle homeotic transformations (48), the axial skeleton of *Rnf2*-HE newborn mice in this study reveals no obvious vertebral transformations or malformations (see Table 1, which is published as supporting information on the PNAS web site, www.pnas.org). In contrast, heterozygocity for Ring1 results in a very strong homeotic phenotype (40). When one *Rnf2* allele is inactivated in addition to both *Bmi1* alleles, only subtle additional changes to the axial skeleton are observed (Table 1). Taken together, the data on axial skeleton development further suggest that Rnf2 cannot compensate for Ring1-dosage variation during somite and vertebral development. Gross morphological appearance and body weight measurements indicate that the *Rnf2*-HE/*Bmi1*-KO mice are delayed in postnatal development at 10 days postpartum, from which point onward growth ceases almost entirely (Fig. 4*a*). In addition, the neurological disorder of *Bmi1*-KO mice (35) is aggravated in *Rnf2*-HE/*Bmi1*-KO mice: animals display a more seriously hampered gait and severe lack of coordination. The molecular and granular layer of the *Rnf2*-HE/*Bmi1*-KO cerebellum are severely depleted at the cellular level, significantly more so than in the *Bmi1*-KO cerebellum (Fig. 4*b C–E*), which may explain the further deterioration of the motoric performance of *Rnf2*-HE/*Bmi1*-KO mice. Poor postnatal development combined with the motor neuron defects results in death at an earlier age than occurs in *Bmi1*-KO animals. The substantially reduced cellularity of the *Rnf2*-HE/*Bmi1*-KO cerebellum (Fig. 4*b C–E*) further indicates that *Ring1* cannot compensate for loss of *Rnf2* on brain development, despite overlap in expression pattern (40). Despite their high homology, mammalian PcG protein homologs are known to have different binding properties to other (PcG) proteins (14). The phenotypic comparison between *Ring1* and *Rnf2* mutant mice further supports the notion of limited functional overlap and target gene specificity between Ring1 or Rnf2-containing PcG complexes in different tissues. The above and related issues will be addressed in an *Rnf2* conditional-KO setting.

Genetic Inactivation of Cdkn2a (Ink4a/ARF) Partially Bypasses the Early Developmental Arrest. The epiblast in most *Rnf2*-KO embryos shows limited expansion, which could point to a proliferative defect. *TrxG* as well as counteracting *PcG* gene products are implicated in cell cycle regulation and malignant transformation (49, 50). Furthermore, Rnf2 and Bmi1 are found in complex with E2F transcription factors, which play key roles in regulation of cellular proliferation and differentiation (51–53). Removal or overexpression of Bmi1 is associated with premature replicative senescence or cellular immortalization and tumorigenesis, respectively (reviewed in ref. 50), an effect that is mediated in part by means of regulation of the *Cdkn2a* locus (33, 54). The Ring finger domain of Bmi1, through which Bmi1 interacts with Rnf2, is essential for Bmi1's oncogenic potential and its ability to mediate cell cycle control by means of the *Cdkn2a* locus (33, 54). This finding prompted us to investigate whether inactivation of *Rnf2* results in derepression of the *Cdkn2a* locus during early development. Indeed, we found expression of $p16^{INK4a}$ up-regulated in *Rnf2*-KO embryos at E7.0 (Fig. 5*a*). To unambiguously demonstrate that *Rnf2* and *Cdkn2a* act

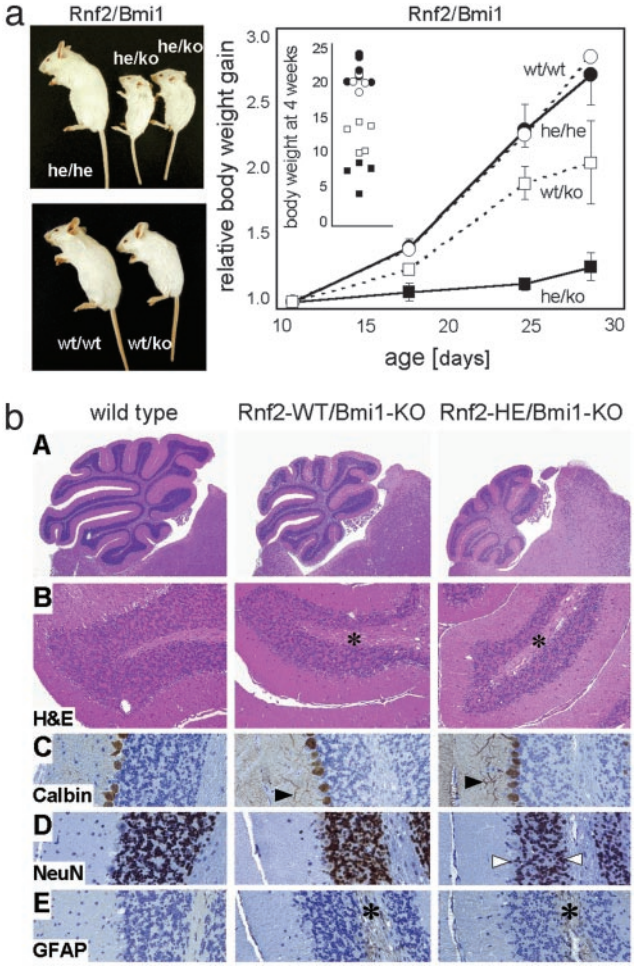

Fig. 4. Genetic interaction of *Rnf2* and *Bmi1* mutations. (*a*) Poor postnatal growth of *Rnf2*-HE/*Bmi1*-KO mice. Gross appearance of *Rnf2*-HE/*Bmi1*-KO (*Upper*) and *Bmi1*-KO (*Lower*) mice at 4 weeks of age as compared with WT and double HE littermates. (*Right*) Postnatal growth curves of *Bmi1*-KO ($n = 2$) and *Rnf2*-HE/*Bmi1*-KO ($n = 2$) mice versus double HE ($n = 4$) and WT ($n = 2$) male littermates and body weight at 4 weeks (*Inset*). Body weight was arbitrarily set at 1 at the time of genotyping (i.e., 10–11 days postpartum). Age at death of *Rnf2*-HE/*Bmi1*-KO was 4–5 weeks. (*b*) Aggravated cerebellar neuropathology in *Rnf2*-HE/*Bmi1*-KO versus *Bmi1*-KO mice. The cerebellum of *Rnf2*-HE/B*mi1*-KO is remarkably smaller (*A*). Both the size and cellularity of the molecular and granular layers are significantly reduced [*B*, hematoxylin and eosin (H&E) staining; *D*, NeuN staining; white arrowheads demarcate the granular layer]. Although reduced in absolute numbers (overall reduction of the cerebellar size), Purkinje cells (PC) fully differentiate as judged by calbindin expression (*C*, calbindin staining) and align well (compare with WT Purkinje cells; *C Left*). Although the orientation of neurites and dendrites is correct, arborization of PC cells in the molecular layer is different: dendrites are thicker and less branched (*C*, black arrowhead). The abnormal arborization, already prevalent in the *Bmi1*-KO, is more pronounced in the *Rnf2*-HE/*Bmi1*-KO cerebellum. Abnormal arborization may be explained by absence of contact and cross talk with molecular neurons during development, which are severely reduced in the *Bmi1*-KO and virtually absent in some cerebellar sections in the *Rnf2*-HE/*Bmi1*-KO (*D*). Both *Bmi1*-KO and *Rnf2*-HE/*Bmi1*-KO cerebellum display distinct gliosis [asterisk in *E*, glial fibrillary acidic protein (GFAP) staining; the asterisk in *B* is an approximate reference point to *E*].

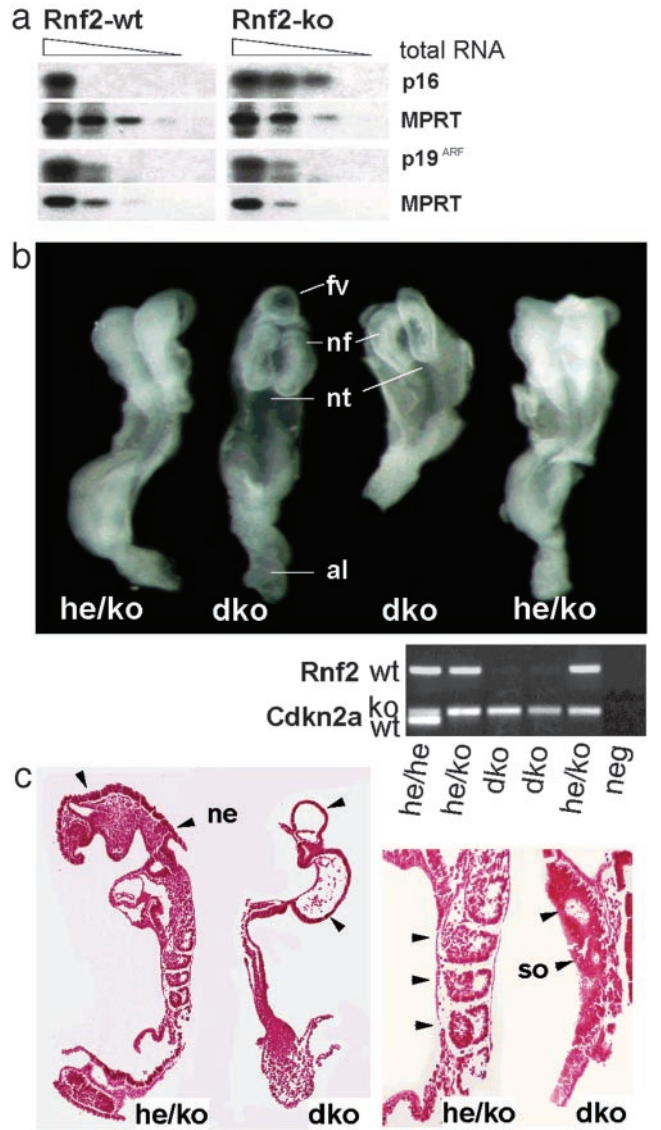

Fig. 5. Partial bypass of the *Rnf2* null mutant developmental arrest by genetic inactivation of the *Cdkn2a* locus. (*a*) Up-regulation of $P16^{INK4a}$ expression in E7.5 embryos as detected by semiquantitative RT-PCR. (*b Upper*) Compared with *Rnf2*-KO embryos, E8 *Rnf2*/*Cdkn2a*-dKO embryos clearly develop further; they are hardly delayed compared with WTs at a similar age; note the well developed neural folds (nf), neural tube (nt), and allantois (al); note also an abnormal frontal neural vesicle (fv) frequently observed in dKO embryos (compare with Fig. 2*a*). *Rnf2*-KO/*Cdkn2a*-KO embryos, however, still do not develop beyond 10–11 days *in utero*. The phenotypes of dKO and of *Rnf2*-HE/*Cdkn2a*-KO embryos (indicated by *he*/*ko*) are compared. DNA from a double heterozygote animal served as a positive control for both the *Cdkn2a*-WT and KO alleles and the *Rnf2*-WT allele (*Lower*). (*c*) Abnormal histology of *Rnf2*-KO/*Cdkn2a*-KO E8.5 embryos. Sagittal sections of dKO embryos confirming abnormal forebrain development in dKO embryos, with a near complete lack of head mesenchyme; the wall of the abnormal frontal vesicle has a neurectoderm-like epithelial structure (ne). Several discernable somites (so), although clearly malformed, indicate paraxial mesoderm formation and segmentation in E8 *Rnf2*/*Cdkn2a*-dKO embryos; cardiac structures were not visible in dKO embryos.

in the same genetic axis, we crossed the *Rnf2* null allele onto the *Cdkn2a*-KO background (36). Genetic removal of the INK4a/ARF cell cycle inhibitors results in a partial rescue of the *Rnf2* null phenotype, and embryonic growth and gastrulation proceed normally until early somite stages (Fig. 5 *b* and *c*). Notably, a number of somites is laid down in paraxial mesoderm of dKO embryos, which is never observed in *Rnf2*-KO embryos (Fig. 5c). Nevertheless dKO embryos still display abnormal morphology and their development does not progress beyond E11–E12. This observation suggests that an INK4a/ARF-activated proliferative block, caused by loss of PcG class II function, clearly contributes to the early developmental arrest in the *Rnf2*-KO.

In summary, we report here that *Rnf2* inactivation is incompat-

ible with early mouse development. In *Rnf2* null mutants, the epiblast fails to expand normally, and mesoderm is not properly laid down or does not migrate anteriorly. Moreover, a clear delay in development of extraembryonic structures accompanies the delay in development of the embryo proper. This condition is reminiscent of the group I PcG *Eed*- and *Ezh2*-mutant phenotype. Although not completely identical to the *Eed* and *Ezh2* null phenotype, the findings indicate that both groups of PcG protein complexes are required from early development onward to maintain correct target gene repression. The gastrulation arrest in the respective null mutant embryos (i.e., *Eed*, *Ezh2*, and *Rnf2*) suggests a mechanistic link between group I and II PcG function in early mammalian development. In mammals and in the fruit fly, Ezh2 and E(z), respectively, were recently uncovered as histone methyl transferases. They are thought to establish silencing through local chromatin structure modification (17): histone methylation by E(z) at lysine-27 in *Drosophila* may subsequently recruit PC, a PRC1 interaction partner of Dring, which recognizes and binds K27Me via its chromodomain (17–19). It is therefore plausible that, early in development, Rnf2-containing protein complexes recognize a preexistent epigenetic repressional state generated by Ezh2 complexes. Alternatively, or possibly additionally, Rnf2 may be involved in mediating a transient group I/II interaction. Recent experiments suggest such a scenario exists in *Drosophila* (55). Elegant experiments in the fruit fly revealed that Esc is required at a transition stage, when early gene silencing is converted into stable repression. This is then maintained by (group II) PRC-1 complexes (56–58). Subsequently it was shown that establishment of heritable Polycomb silencing requires a transient interaction between class I and II proteins during the first 3 h of embryonic development (59). It is conceivable that a similar interaction takes place during early mammalian development. Finally, in analogy with the central position of Dring in the *Drosophila* PRC-1 core-complex formation (60) Rnf2 may function as a crucial assembly factor in mammalian PRC complexes (20). Failure to assemble PcG complexes will result in derepression of critical target genes and subsequent developmental arrest. We show here that Rnf2-mediated repression of the *Cdkn2a* (*Ink4a/ARF*) locus is crucial for early development to proceed normally. This observation may be part of a mechanism ensuring heritable transcriptional maintenance during the rapid cell divisions that occur before and during early gastrulation. Besides a role in differentiation and determination, these data establish an important function for PcG proteins in cell cycle regulation in early mammalian development.

We are indebted to M. Dyer and H. Koseki for Ring1b antiserum; A. Ullrich for the Ezh2 antiserum; M. Djabali for *Cbx2* cDNA; T. Jenuwein for *Ezh2* cDNAs; M. Vidal for *Ring1* and *Rnf2* expression vectors; A. Schumacher for an *Evx-1* probe and *Eed* cDNA; B. Herrmann, R. Krumlauf, and E. De Robertis for *Brachyury T*, *Hoxb1*, and *mCer1* probes, respectively; and M. Serrano and R. DePinho for *Cdkn2a* (*Ink4a/ARF*) null mutant mice. We thank J. Korving, E. Boutsma, K. van Veen, E. Wientjes, and K. Kieboom for excellent technical assistance; A. Beverdam, F. Meijlink, R. Carvalho, and S. Chuva de Sousa Lopes for help with *in situ* hybridizations; L. Oomen for help with graphical work; and K. Lawson, A. Lund, R. Zwart, and R. Kingston for critical discussion. J.W.V. was supported by a grant from the Dutch Organization for Scientific Research.

1. Paro, R. (1990) *Trends Genet*. **6,** 416–421.
2. Kennison, J. A. (1995) *Annu. Rev. Genet*. **29,** 289–303.
3. Simon, J. (1995) *Curr. Opin. Cell Biol*. **7,** 376–385.
4. Pirrotta, V. (1998) *Cell* **93,** 333–336.
5. Lewis, E. B. (1978) *Nature* **276,** 565–570.
6. Krumlauf, R. (1994) *Cell* **78,** 191–201.
7. Deschamps, J., van den Akker, E., Forlani, S., De Graaff, W., Oosterveen, T., Roelen, B. & Roelfsema, J. (1999) *Int. J. Dev. Biol*. **43,** 635–650.
8. Sewalt, R. G., van der Vlag, J., Gunster, M. J., Hamer, K. M., den Blaauwen, J. L., Satijn, D. P., Hendrix, T., van Driel, R. & Otte, A. P. (1998) *Mol. Cell. Biol*. **18,** 3586–3595.
9. van Lohuizen, M., Tijms, M., Voncken, J. W., Schumacher, A., Magnuson, T. & Wientjens, E. (1998) *Mol. Cell. Biol*. **18,** 3572–3579.
10. Alkema, M. J., Bronk, M., Verhoeven, E., Otte, A., van't Veer, L. J., Berns, A. & van Lohuizen, M. (1997) *Genes Dev*. **11,** 226–240.
11. Gunster, M. J., Satijn, D. P., Hamer, K. M., den Blaauwen, J. L., de Bruijn, D., Alkema, M. J., van Lohuizen, M., van Driel, R. & Otte, A. P. (1997) *Mol. Cell. Biol*. **17,** 2326–2335.
12. Korf, I., Fan, Y. & Strome, S. (1998) *Development (Cambridge, U.K.)* **125,** 2469–2478.
13. Grossniklaus, U., Vielle-Calzada, J. P., Hoeppner, M. A. & Gagliano, W. B. (1998) *Science* **280,** 446–450.
14. Satijn, D. P. & Otte, A. P. (1999) *Biochim. Biophys. Acta* **1447,** 1–16.
15. Brock, H. W. & van Lohuizen, M. (2001) *Curr. Opin. Genet. Dev*. **11,** 175–181.
16. van der Vlag, J. & Otte, A. P. (1999) *Nat. Genet*. **23,** 474–478.
17. Cao, R., Wang, L., Wang, H., Xia, L., Erdjument-Bromage, H., Tempst, P., Jones, R. S. & Zhang, Y. (2002) *Science* **298,** 1039–1043.
18. Czermin, B., Melfi, R., McCabe, D., Seitz, V., Imhof, A. & Pirrotta, V. (2002) *Cell* **111,** 185–196.
19. Muller, J., Hart, C. M., Francis, N. J., Vargas, M. L., Sengupta, A., Wild, B., Miller, E. L., O'Connor, M. B., Kingston, R. E. & Simon, J. A. (2002) *Cell* **111,** 197–208.
20. Levine, S. S., Weiss, A., Erdjument-Bromage, H., Shao, Z., Tempst, P. & Kingston, R. E. (2002) *Mol. Cell. Biol*. **22,** 6070–6078.
21. Sewalt, R. G., Lachner, M., Vargas, M., Hamer, K. M., den Blaauwen, J. L., Hendrix, T., Melcher, M., Schweizer, D., Jenuwein, T. & Otte, A. P. (2002) *Mol. Cell. Biol*. **22,** 5539–5553.
22. Hemenway, C. S., Halligan, B. W. & Levy, L. S. (1998) *Oncogene* **16,** 2541–2547.
23. Schoorlemmer, J., Marcos-Gutierrez, C., Were, F., Martinez, R., Garcia, E., Satijn, D. P., Otte, A. P. & Vidal, M. (1997) *EMBO J*. **16,** 5930–5942.
24. Satijn, D. P., Gunster, M. J., van der Vlag, J., Hamer, K. M., Schul, W., Alkema, M. J., Saurin, A. J., Freemont, P. S., van Driel, R. & Otte, A. P. (1997) *Mol. Cell. Biol*. **17,** 4105–4113.
25. Wilkinson, D. G., Bailes, J. A., Champion, J. E. & McMahon, A. P. (1987) *Development (Cambridge, U.K.)* **99,** 493–500.
26. Vogels, R., de Graaff, W. & Deschamps, J. (1990) *Development (Cambridge, U.K.)* **110,** 1159–1168.
27. Wilkinson, D. G., ed. (1992) *In Situ Hybridization: A Practical Approach* (IRL, Oxford).
28. Morgenstern, J. P. & Land, H. (1990) *Nucleic Acids Res*. **18,** 3587–3596.
29. Kinsella, T. M. & Nolan, G. P. (1996) *Hum. Gene Ther*. **7,** 1405–1413.
30. Rigaut, G., Shevchenko, A., Rutz, B., Wilm, M., Mann, M. & Seraphin, B. (1999) *Nat. Biotechnol*. **17,** 1030–1032.
31. Chomczynski, P. & Sacchi, N. (1987) *Anal. Biochem*. **162,** 156–159.
32. Voncken, J. W., Griffiths, S., Greaves, M. F., Pattengale, P. K., Heisterkamp, N. & Groffen, J. (1992) *Cancer Res*. **52,** 4534–4539.
33. Jacobs, J. J., Kieboom, K., Marino, S., DePinho, R. A. & van Lohuizen, M. (1999) *Nature* **397,** 164–168.
34. Bel, S., Core, N., Djabali, M., Kieboom, K., van der Lugt, N., Alkema, M. J. & van Lohuizen, M. (1998) *Development (Cambridge, U.K.)* **125,** 3543–3551.
35. van der Lugt, N. M., Domen, J., Linders, K., van Roon, M., Robanus-Maandag, E., te Riele, H., van der Valk, M., Deschamps, J., Sofroniew, M., van Lohuizen, M., *et al*. (1994) *Genes Dev*. **8,** 757–769.
36. Serrano, M., Lee, H., Chin, L., Cordon-Cardo, C., Beach, D. & DePinho, R. A. (1996) *Cell* **85,** 27–37.
37. Akasaka, T., Kanno, M., Balling, R., Mieza, M. A., Taniguchi, M. & Koseki, H. (1996) *Development (Cambridge, U.K.)* **122,** 1513–1522.
38. Core, N., Bel, S., Gaunt, S. J., Aurrand-Lions, M., Pearce, J., Fisher, A. & Djabali, M. (1997) *Development (Cambridge, U.K.)* **124,** 721–729.
39. Takihara, Y., Tomotsune, D., Shirai, M., Katoh-Fukui, Y., Nishii, K., Motaleb, M. A., Nomura, M., Tsuchiya, R., Fujita, Y., Shibata, Y., *et al*. (1997) *Development (Cambridge, U.K.)* **124,** 3673–3682.
40. del Mar Lorente, M., Marcos-Gutierrez, C., Perez, C., Schoorlemmer, J., Ramirez, A., Magin, T. & Vidal, M. (2000) *Development (Cambridge, U.K.)* **127,** 5093–5100.
41. Akasaka, T., van Lohuizen, M., van der Lugt, N., Mizutani-Koseki, Y., Kanno, M., Taniguchi, M., Vidal, M., Alkema, M., Berns, A. & Koseki, H. (2001) *Development (Cambridge, U.K.)* **128,** 1587–1597.
42. Schumacher, A., Faust, C. & Magnuson, T. (1996) *Nature* **383,** 250–253.
43. O'Carroll, D., Erhardt, S., Pagani, M., Barton, S. C., Surani, M. A. & Jenuwein, T. (2001) *Mol. Cell. Biol*. **21,** 4330–4336.
44. Wang, J., Mager, J., Chen, Y., Schneider, E., Cross, J. C., Nagy, A. & Magnuson, T. (2001) *Nat. Genet*. **28,** 371–375.
45. Faust, C., Lawson, K. A., Schork, N. J., Thiel, B. & Magnuson, T. (1998) *Development (Cambridge, U.K.)* **125,** 4495–4506.
46. Faust, C., Schumacher, A., Holdener, B. & Magnuson, T. (1995) *Development (Cambridge, U.K.)* **121,** 273–285.
47. Belo, J. A., Bouwmeester, T., Leyns, L., Kertesz, N., Gallo, M., Follettie, M. & De Robertis, E. M. (1997) *Mech. Dev*. **68,** 45–57.
48. Suzuki, M., Mizutani-Koseki, Y., Fujimura, Y., Miyagishima, H., Kaneko, T., Takada, Y., Akasaka, T., Tanzawa, H., Takihara, Y., Nakano, M., *et al*. (2002) *Development (Cambridge, U.K.)* **129,** 4171–4183.
49. Caldas, C. & Aparicio, S. (1999) *Cancer Metastasis Rev*. **18,** 313–329.
50. Jacobs, J. J. & van Lohuizen, M. (2002) *Biochim. Biophys. Acta* **1602,** 151–161.
51. Trimarchi, J. M., Fairchild, B., Wen, J. & Lees, J. A. (2001) *Proc. Natl. Acad. Sci. USA* **98,** 1519–1524.
52. Ogawa, H., Ishiguro, K., Gaubatz, S., Livingston, D. M. & Nakatani, Y. (2002) *Science* **296,** 1132–1136.
53. Dahiya, A., Wong, S., Gonzalo, S., Gavin, M. & Dean, D. C. (2001) *Mol. Cell* **8,** 557–569.
54. Alkema, M. J., Jacobs, H., van Lohuizen, M. & Berns, A. (1997) *Oncogene* **15,** 899–910.
55. Beuchle, D., Struhl, G. & Muller, J. (2001) *Development (Cambridge, U.K.)* **128,** 993–1004.
56. Struhl, G. (1981) *Nature* **293,** 36–41.
57. Struhl, G. & Brower, D. (1982) *Cell* **31,** 285–292.
58. Duncan, I. M. (1982) *Genetics* **102,** 49–70.
59. Poux, S., Melfi, R. & Pirrotta, V. (2001) *Genes Dev*. **15,** 2509–2514.
60. Francis, N. J., Saurin, A. J., Shao, Z. & Kingston, R. E. (2001) *Mol. Cell* **8,** 545–556.
61. Frohman, M. A., Boyle, M. & Martin, G. R. (1990) *Development (Cambridge, U.K.)* **110,** 589–607.